

Differential methylation of G-protein coupled receptor signaling genes in gastrointestinal neuroendocrine tumors

Seyoun Byun

University of Utah

Kajsa E. Affolter

University of Utah

Angela K. Snow

University of Utah

Karen Curtin

University of Utah

Austin R. Cannon

University of Utah

Lisa A. Cannon-Albright

University of Utah

Ramya Thota

Intermountain Healthcare

Deborah W. Neklason (✉ deb.neklason@hci.utah.edu)

University of Utah

Research Article

Keywords: Neuroendocrine, small intestine, gastrointestinal, DNA methylation, carcinoid, G-protein coupled receptor, TRHR, SST

Posted Date: February 23rd, 2021

DOI: <https://doi.org/10.21203/rs.3.rs-224809/v1>

License: © ⓘ This work is licensed under a Creative Commons Attribution 4.0 International License.

[Read Full License](#)

Abstract

Neuroendocrine tumors (NETs) of the small intestine undergo large chromosomal and methylation changes. The objective of this study was to identify methylation differences in NETs and consider how the differentially methylated genes may impact patient survival. Whole genome methylation and chromosomal copy number variation (CNV) of NETs from the small intestine and appendix was measured. Tumors were divided into three molecular subtypes according to CNV results: chromosome 18 loss (18LOH), MultiCNV, and NoCNV. Comparison of 18LOH tumors with MultiCNV and NoCNV tumors identified 901 differentially methylated genes which are over represented with seven G-protein coupled receptor (GPCR) pathways and the gene encoding somatostatin (*SST*), a clinical target for NETs. Patient survival based on low versus high methylation in all samples identified four significant genes ($p < 0.05$) *OR2S2*, *SMILR*, *RNU6-653P* and *AC010543.1*. Within the 18LOH molecular subtype tumors, survival differences were identified in high versus low methylation of 24 genes. The most significant is *TRHR* ($p < 0.01$), a GPCR with multiple FDA-approved drugs. By separating NETs into different molecular subtypes based on chromosomal changes, we find that multiple GPCRs and their ligands appear to be regulated through methylation and correlated with survival. Opportunities for better treatment strategies based on molecular features exist for NETs.

Statement Of Significance

Gastrointestinal neuroendocrine tumors are rare and the molecular pathology is poorly defined. G-protein coupled receptors and ligands are regulated through methylation and correlated with survival. This presents opportunities to develop better treatments.

Introduction

Well differentiated neuroendocrine tumors (NETs), previously referred to as carcinoids, can occur anywhere in the body, with the majority occurring in the gastrointestinal tract. Small intestinal NETs make up almost half of these gastrointestinal NETs (GINETs) and are rare, with an incidence of 0.87 per 100,000 population per year¹⁻³. Since GINETs are rare cancers, the molecular mechanisms driving pathologic changes remain elusive. Small intestinal NETs arise from enterochromaffin cells, which reside alongside the epithelial layer lining the lumen of the digestive tract, predominantly in the small intestine and appendix, where they regulate intestinal motility and secretion via production of serotonin and other peptides^{4,5}. Excess production of serotonin by the tumor may cause carcinoid syndrome, characterized by flushing and diarrhea, which is found in about 17% of appendiceal and 32% of small intestinal NETs⁶.

GINETs often express neuroendocrine markers, such as synaptophysin, chromogranin and somatostatin receptors (SSTRs) 1 to 5, which are G-protein coupled receptors and detected by immunohistochemistry. The positron emission tomography (PET) imaging using radiolabeled SSTR ligand tracers such as ⁶⁸Ga-DOTATE and ⁶⁸Ga-DOTATOC is a highly sensitive modality to diagnose patients with local or distant well-differentiated GINETs and also to evaluate for the potential role of somatostatin analogue (SSA) therapy

(octreotide or lanreotide) in patients with metastatic NETs^{7,8}. SSAs regulate hormonal hypersecretion, notably serotonin and other vasoactive substances in tumors expressing one or more subtypes of somatostatin receptors. Currently, metastatic GINETs are treated with the standard first-line SSA therapy, but there is evidence that different molecular subtypes are associated with different progression-free survival⁹. A better understanding of the molecular characteristics underlying GINETs may provide guidance for understanding the biology, prognosis and better selection of patients for more effective and targeted treatments.

The most frequent genomic alteration in small intestinal NETs is large chromosomal deletions. Most notably, full arms of chromosomes 18 are lost in 40–80% of tumors^{10–12}. Inactivating mutations in *CDKN1B* are found in about 8% of small intestinal NETs, but small intestinal NETs otherwise are genetically stable, and somatic mutations in individual genes are not common^{13,14}. Epigenetic modifications, in particular DNA methylation, have been proposed as a mechanism for small intestinal NET development⁹. DNA methylation can regulate gene expression and is an established mechanism for the development of multiple types of cancer¹⁵. In general, but not exclusively, hypermethylation in promoter regions tends to decrease gene expression by blocking DNA binding sites for transcription factors^{16,17}.

Multiple studies have considered the clinical significance of loss of heterozygosity in chr18 (18LOH) with inconsistent results¹⁸. Karpathakis et al. suggested that small intestinal NETs with 18LOH are associated with worse overall survival. Yao et al. reported the 18LOH patients have better survival outcomes¹⁰. Kim et al. found no significant difference in overall survival between those with and without 18LOH small intestinal NETs¹⁹. Although there is evidence of methylation changes in small intestinal NETs with 18LOH, the molecular pathways are not well defined⁹.

The objective of this study was to identify methylation differences in small intestinal and appendiceal NETs based on genomic alteration (molecular subtype) and to consider how the differentially methylated genes may impact survival.

Materials And Methods

All methods were carried out in accordance with relevant guidelines and regulations. The study was approved by the University of Utah Institutional Review Board. Informed consent was obtained from all living participants.

Research Participants

Potential NET patient cases including both small intestine and appendix (histology codes 8240, 8241, 8243, 8244, 8246; ICDO locations 170, 171, 172, 173, 178, 179, 181) in Utah between 1999 and 2014 were identified through the Utah Cancer Registry (UCR). Cases from subjects under 18 years old and *in situ* cases were excluded, leaving 552 potential NET subjects for study (Table 1). Additional cases with a

diagnosis from 2014 to 2018 were identified through University of Utah Health electronic medical records and referred to the study by the Department of Surgery. UCR referred 77 cases which had been reported to UCR by University of Utah Health and had a pathology number on record. The Department of Surgery referred 12 additional recent cases. From these 89 cases, 47 subjects had archived FFPE blocks available, were confirmed as a well-differentiated neuroendocrine tumor by study pathologist (KA), and had sufficient tissue for methylation analysis.

TABLE 1: Characteristics of NET cases tested

	Cases tested	Cases not tested	<i>p</i>
Number	47	516	
Diagnosis Years	1999-2018	1999-2014	
Male	28 (59.6%)	285 (55.2%)	0.33*
Average age at diagnosis (range)	60.6 (25-87)	62.1 (19-90)	0.45 [^]
Tumor location			
Small intestine (170-173, 178, 179)	44 (93.6%)	475 (92.1%)	
Appendix (181)	3 (6.4%)	41 (7.9%)	0.33*
Stage			
Localized (1)	12 (25.5%)	170 (32.9%)	
Regional (2,3,4)	23 (48.9%)	224 (43.4%)	
Distant (7)	12 (25.5%)	110 (21.3%)	
Unstaged (9)	0	12 (2.3%)	0.80*
Grade			
Grade 1	26 (70.3%)	155 (69.2%)	
Grade 2	10 (27.0%)	59 (26.3%)	
Grade 3	1 (2.7%)	10 (4.5%)	0.61*
Total tumors graded	37 (78.7%)	224 (43.4%)	
Unknown grade	10 (21.3%)	292 (56.6%)	0.49*
Tobacco use indication	13 (27.6%)	159 (30.8%)	0.33*
Family history of SINT	1 (2.1%)	14 (2.7%)	0.32*

*Chi-square test used; [^] Student's t-test used

Methylation analysis of tumor DNA

Formalin-fixed paraffin-embedded (FFPE) blocks were serially cut in 5 µm increments and mounted onto charged slides. Hematoxylin and eosin (H&E) staining of a representative slide was used to identify areas of neuroendocrine tumor (> 50% tumor) by the study pathologist (KA). Cells were microdissected from the marked tumor region, and DNA was extracted from FFPE tissue slides using a QIAamp DNA FFPE Tissue Kit [Qiagen #56404] using the manufacturer's protocol with the following modifications: (1) paraffin was removed from the slides prior to microdissection, and the tissue was added directly to Buffer ATL (2) there were two 56°C incubations with Proteinase K: overnight, and then for an hour after supplementing

with an additional 20 μ L Proteinase K (3) for the elution, 2 x 25 μ L of ATE was added to the center of the membrane and incubated for 5 minutes at room temperature before eluting.

Following extraction, DNA concentrations were measured with a Qubit™ dsDNA BR assay kit [ThermoFisher Scientific #Q32850 & #Q32856]. Bisulfite conversion was performed on 250 ng DNA per sample using a Zymo EZ DNA Methylation Kit [Zymo Research #D5001] following the manufacturer's recommended protocol for methylation microarrays. DNA quality was evaluated with an Infinium FFPE QC kit [Illumina #WG-321-1001] prior to performing the recommended FFPE DNA Restore protocol [Illumina #WG-321-1002 & Zymo #D4024]. MethylationEPIC BeadChip microarrays [Illumina #WG-317-1002] were used for genome-wide methylation profiling. The microarrays were processed with an Illumina iScan platform using the Infinium HD Methylation assay protocol with the recommended modifications for FFPE samples. The raw methylation IDAT data was analyzed using GenomeStudio (RRID:SCR_010973) v2011.1 software with Methylation Module v1.9 [Illumina].

DNA methylation data pre-processing

The methylation data were pre-processed following a pipeline of the ChAMP (RRID:SCR_012891) R package (V.2.13.5)²⁰. Probes were filtered out using the *champ.filter* function with following criteria: probes with [1] detection $p > 0.01$, [2] less than three beads in at least 5% of samples, [3] non-CpG cytosine, [4] polymorphic nucleotide, [5] multiple regions of the genome and [6] chromosome X, and Y. Total of the 699,602 CpG sites were selected for further analysis. After the quality control, the type-II probe bias was corrected by the method of beta mixture quantile (BMIQ) normalization according to pipeline defaults.

Copy number variants using methylation data

In order to identify copy number variation (CNV) in our 47 NET cases, methylation status of our NETs was compared with previously published Illumina MethylationEPIC BeadChip data measured from ten normal myometrial samples in NCBI GEO database (GSM3417135-GSM3417144)²¹. CNV was estimated and compared from the methylation beta value using the *champ.CNA* function of ChAMP. The whole-chromosome arm CNV was defined with the criteria of length $> 80\%$ and segment mean $> \pm 0.2$. In addition, the 47 NETs were classified into three groups according to CNV results: Chromosome 18 LOH (18LOH), no considerable copy number alterations (NoCNV), and multiple copy number alterations (MultiCNV).

Differential methylation analysis

In three groups according to CNV results, the averaged methylation value (β -value) of all CpGs was compared within the promoter region pairwise (i.e., 18LOH vs. NoCNV, 18LOH vs. MultiCNV, and MultiCNV vs. NoCNV) with an unpaired Wilcoxon's test to identify genes with differential methylation status. The promoter region was considered as 1500 bp upstream and 200 bp downstream from the transcription start site (TSS). A total of 39,252 genes were tested. An FDR adjusted p-value below 0.05 and $\Delta\beta > 0.15$ were used to identify genes with statistically significant differential methylation levels.

Functional enrichment and network analysis

Functional enrichment analysis using ConsensusPathDB (RRID:SCR_002231) (Release 33, CPDB; <http://cpdb.molgen.mpg.de/>)²² was used to interpret the functional role of genes identified with differential methylation status. Significant pathways and GO terms were defined as having an adjusted q -value < 0.05 (p -value corrected for multiple testing based on number of pathways used). To reduce redundancy and remove potential false positive GO terms, we used GO-module web-tool (<http://lussierlab.org/GO-Module>) (v.1.3)²³. Protein-protein interaction (PPI) network was constructed using StringDB V.11 (STRING, RRID:SCR_005223, <http://string-db.org>)²⁴ with an interaction combined score of > 0.9 which represents the highest confidence score of the various evidence (i.e., text mining, database, and co-expression). PPI network was visualized by using Cytoscape (RRID:SCR_003032) v3.5.1²⁵.

Survival analysis

Survival in months after diagnosis was determined from death certificates ($n = 16$). If the individual was alive at last contact ($n = 31$), a study-end month was set at June 2019, the most recent contact date among research subjects.

Overall survival outcome was evaluated using Kaplan-Meier survival analysis with several comparing criteria. Analyses were conducted according to the three molecular subgroups (i.e., 18LOH, NoCNV, and MultiCNV). We also considered survival based on methylation status of gene promoters ($n = 39,252$ genes including coding, non-coding, and pseudogenes). The 47 NET samples were separated into two groups according to β -value (i.e., low- and high-methylated groups) using k -means clustering. Survival analysis of the 18LOH tumors ($n = 19$) separated into two groups according to β -value was done for the 901 differentially methylated genes. We defined statistically significant associations as a p -value < 0.05 .

Results

Overview of the study cohort

Although the number of tumors tested for methylation (1999–2018) was modest, this subset was generally representative of all small intestine and appendix NET cases reported to the UCR in 1999–2014 (Table 1). In those cases with testing, a larger percentage had tumor grade information available: 79% versus 43% of the cases who did not undergo testing. This is expected because the cases tested, on average, were more recent diagnoses and came from an academic institution where tumor grading was more common. Restricting the comparison to tumors that were graded, the tumors tested versus tumors of cases that were not tested were similar in frequency of grade, with the majority (70% and 69%, respectively) being grade 1. Known risk factors of tobacco use and family history were similar between cases with and without testing as well. Survival did not significantly differ between the two groups ($p = 0.76$; Supplementary Fig. S1).

Genome-wide DNA methylation copy number variation profiling

Analysis of copy number variation (CNV) in the tumor, based on DNA methylation array data, showed losses on the entire chromosome 18 (18LOH) in 19 out of 47 tumors (40.4%) and loss of chromosome 5 in 5 tumors (10.6%), similar to previous reports²⁶⁻²⁸. Multiple CNV (MultiCNV) were observed in 8 tumors (17.0%), and no copy number alternation (NoCNV) was observed in the remaining 20 tumors (42.6%), three of which are from the appendix (NoCNV_6, NoCNV_7, NoCNV_8; Fig. 1).

Differential DNA methylation analysis in the three subgroups

A subset of 196,354 CpG methylation sites out of a total of 699,602 CpG sites was mapped to specific promoters (39,252 genes) for analysis (Fig. 2a). To identify differentially methylated genes related to 18LOH, intergroup comparisons were performed for 18LOH vs. MultiCNV, 18LOH vs. NoCNV, and MultiCNV vs. NoCNV (FDR < 0.05 and $\Delta\beta > 0.15$); the number of differential methylated genes are 1332, 1259, and 0, respectively. (Fig. 2b). An intersection of 901 genes was differentially methylated in the 18LOH group. Interestingly, 205 (22.8%) of the 901 differentially methylated genes were annotated as long non-coding RNA (lncRNA). Heatmap clustering of the 901 genes shows that these genes are predominately hypomethylated in 18LOH tumors when compared to MultiCNV and NoCNV groups. (Fig. 2c). Only 9 genes (1%) were hypermethylated in the 18LOH tumors (*SST*, *DMBT1*, *RNU6-1039P*, *RP11-37N22.1*, *Lnc-FAM241A-1*, *RP11-153K16.1*, *CERS3-AS1*, *RP11-542M13.3*, and *AC025278.2*; Fig. 2c). Hierarchical clustering of the tumors based on methylation of the 901 genes shows separation of the small intestinal 18LOH tumors from the other two molecular subtypes (Fig. 2d). The three tumors identified by ICDO 181 (appendix) cluster with the NoCNV molecular subtype.

Functional enrichment analysis and network of significant methylated of ch18 LOH tumors

Overrepresentation analysis of the 901 genes, using ConsensusPathDB, revealed 12 enriched functional pathways (q-value < 0.05) (Supplementary Fig. S2). This includes multiple signaling-related pathways: GPCR signaling (including olfactory receptors), defensin and beta-defensin, neuroactive ligand-receptor interaction, vitamin D receptor, and hemostasis. Within the set of 901 differentially methylated genes, 18 Gene Ontology (GO) pathways were significantly over-represented (q-value < 0.05), including "Olfactory receptor activity" (GO:0004984), "Sensory perception of chemical stimulus" (GO:0007606), "G-protein-coupled receptor signaling pathway" (GO:0004930), "defense response to bacterium" (GO:0042742), and "humoral immune response" (GO:0006959) (Supplementary Fig. S2). The protein-protein interaction (PPI) network constructed with STRING database identified 51 genes with direct interactions (Fig. 3). When genes from the 12 enriched functional pathways were superimposed on the PPI network, the 51 genes were functionally grouped into four subgroup pathways: GPCR downstream signaling (including olfactory

receptors), neuroactive ligand-receptor interaction, beta-defensins, and hemostasis. The GPCR downstream signaling pathway is highly related to cancer progression behaviors such as proliferation, angiogenesis, and metastasis^{29–31}. Multiple genes were assigned to both GPCR and neuroactive ligand-receptor interaction pathways.

When tumors were grouped into high methylation versus low methylation for all 39,252 genes, four genes were identified with significance $p < 0.05$: *OR2S2*, *SMILR*, *RNU6-653P* and *AC010543.1*. Conflicting reports on the survival benefit with 18LOH tumors may represent heterogeneity in methylation, thus survival for high versus low methylation was considered within this group of 19 tumors for the 901 differentially methylated genes. A significant difference in survival ($p < 0.05$) was observed for 24 of the genes (Supplementary Table S1). Two are included in the PPI network (Fig. 3): *TRHR* ($p = 0.006$) and *VNN2* ($p = 0.050$).

By way of example, two genes whose methylation may have biological importance in neuroendocrine tumors are highlighted with additional detail; *TRHR* (thyrotropin releasing hormone receptor), a G-protein coupled receptor, and *SST* (somatostatin), a ligand to the *SSTR* G-protein coupled receptor. The *TRHR* promoter is hypomethylated on all six CpG methylation sites in tumors with 18LOH relative to tumors with NoCNV ($p = 0.004$) or with MultiCNV ($p = 0.04$) (Fig. 4a and 4b). Survival analysis of the 18LOH tumors suggests that low methylation of the *TRHR* gene confers poor survival $p = 0.005$ (Fig. 4c). Methylation of the *TRHR* promoter silences transcription of the gene in thyroid cancers³². This suggests that reduced *TRHR* expression due to promoter methylation improves survival.

The *SST* promoter is hypermethylated in the 18LOH tumors relative to the MultiCNV ($p = 0.006$) and NoCNV ($p = 0.002$) tumors (Fig. 5a and 5b). Hypermethylation of the *SST* promoter in gastric cancers results in decreased mRNA and protein expression, thereby reducing somatostatin's ability to inhibit tumor growth³³. The somatostatin protein binds to G-protein coupled somatostatin receptors, and analogs of somatostatin are a common treatment for GINETS⁸.

Discussion

In this study, we investigated differential DNA methylation status in well-differentiated small intestinal and appendiceal NETs with different molecular subtypes. We found 901 genes with differentially methylated promoter regions in the study's NETs having 18LOH, and these genes were enriched in tumor-related pathways, including "GPCR downstream signaling," "neuroactive ligand-receptor interaction," "beta defensins," and "hemostasis". Most of the genes were hypomethylated, broadly suggesting transcriptional activation of these genes. The lncRNA, which made up 22.8% of the differentially methylated genes, have been shown to regulate cancer genes and may represent additional disease pathways^{34–37}.

The GPCR pathway represents a large family of cell-surface molecules regulating the signal transmission for multiple cellular functions. GPCRs are also the most common class of therapeutic targets, with

approximately 700 FDA-approved drugs targeting 128 GPCRs^{38,39}. Pertinent to the findings of this study, GPCRs play multiple roles in cancer development and have been the focus of past studies to define differences in neuroendocrine tumors, primarily those originating from the small intestine versus pancreas and lung^{40,41}. Our significantly enriched GPCR pathway suggests that expression of GPCR pathways are controlled through methylation events which in turn drive tumor progression a subset of GINETS^{41,42}. Being neuroendocrine tumors, it makes sense that the 'neuroactive ligand-receptor interaction' pathway is involved, and accordingly, is part of the GPCR downstream signaling pathway. We describe hypermethylation of one such neuroactive ligand, the *SST* gene encoding somatostatin, in 18LOH tumors relative to NoCNV and MultiCNV. Somatostatin is the ligand for SSTRs, G-protein coupled somatostatin receptors that are overexpressed in a subset of GINETS and the target of somatostatin analog therapies. Examining the clinical response to somatostatin analog therapies relative to *SST* methylation state may provide guidance on more targeted treatment strategies.

Our survival analysis with the three molecular subgroups based on chromosomal changes showed there was no significant difference between subgroups ($p = 0.41$; supplementary Fig. S3) However, the ability to detect such differences is limited by the sample size. We did identify 24 genes with methylation levels associated with survival outcomes specifically in 18LOH tumors, potentially explaining why there is disagreement in the literature on survival benefits for 18LOH tumors. The most significant association was with *TRHR*. Hypomethylation of the *TRHR* promoter may be associated with 18LOH tumor progression and survival outcomes. The mechanism behind this survival difference is not obvious but may represent a constellation of methylation events that are clinically relevant, potentially as a pharmacologic target for small intestinal NET patients.

Selection of tumors from the cancer registry included ICDO codes for the small intestine as well as the appendix because we believe there is cross-over in the etiology of these tumors. Three of the 47 tumors examined for methylation were from the appendix. All three were classified as NoCNV subtype, and hierarchical clustering of their methylation profile was fully integrated with the other NoCNV samples from the small intestine, suggesting a similar etiology. Additionally, we have observed neuroendocrine tumors of the appendix in families with multiple NETs of the small intestine, which suggests there is overlap in the genetic etiology.

Limitations of the study included small sample size, methylation arrays were not run on matched normal tissues and a lack of treatment data for the NET patients. Also, the methylation changes were not validated with RNA expression profiling, but rather relied on published results in different tissues. Strengths are that the samples tested were representative of all tumors reported in the state for that period of time, and that the frequency of molecular subtypes were similar to previous reports^{9,11-13}.

In conclusion, by separating small intestine and appendiceal NETs into different molecular subtypes based on chromosomal changes, we were able to define major pathways that are differentially methylated. Two relevant pathways were the GPCR and the overlapping neuroactive ligand-receptor interaction. One gene that is differentially hypermethylated in 18LOH tumors is *SST*, encoding

somatostatin. Somatostatin analogs are a primary treatment for GINETs, targeting overexpressed somatostatin receptors on the tumors. Somatostatins are also used for GINET visualization, radiotherapy, and repressing carcinoid-syndrome side effects. GPCR may be important for survival in small intestinal NETs and are targetable by drugs in some cases. In future work, methylation status in these genes can be explored as a prognostic and/or predictive biomarker to predict responses to SSA's and for careful selection of patients for appropriate treatments. Future studies that incorporate detailed histologic characterization, GPCR expression, and treatments will be important. The molecular characterization of GINETs can lead to novel prognostic and predictive biomarkers to better inform treatments and may improve survival of patients with GINETs.

Declarations

Acknowledgments

We gratefully acknowledge support from the Center for High Performance Computing and the Genomics Core Facility at the University of Utah and the Utah Population Database. We would like to acknowledge Megan Keener for assisting with sample acquisition and Joshua Unger and Greyson Hullinger for processing the tumor samples.

Financial Support: This work was supported by grants from the National Cancer Institute at the National Institutes of Health, R21CA205796 (DWN) and P30CA042014 and Huntsman Cancer Foundation. Support for the Utah Cancer Registry is provided by Contract #HHSN 261201000026C from the National Cancer Institute with additional support from the Utah Department of Health and the University of Utah. Support for the computational resources at the Center for High Performance Computing at the University of Utah were partially funded by the NIH Shared Instrumentation Grant 1S100D021644-01A1.

Conflict of Interest Statement: The authors have no conflicts of interest to disclose.

References

1. Modlin, I. M., Lye, K. D. & Kidd, M. A 5-decade analysis of 13,715 carcinoid tumors. *Cancer*. **97**, 934–959 <https://doi.org/10.1002/cncr.11105> (2003).
2. DiSario, J. A., Burt, R. W., Vargas, H. & McWhorter, W. P. Small bowel cancer: epidemiological and clinical characteristics from a population-based registry. *Am J Gastroenterol*. **89**, 699–701 (1994).
3. Kharazmi, E., Pukkala, E., Sundquist, K. & Hemminki, K. Familial risk of small intestinal carcinoid and adenocarcinoma. *Clin Gastroenterol Hepatol*. **11**, 944–949 <https://doi.org/10.1016/j.cgh.2013.02.025> (2013).
4. Bertrand, P. P. & Bertrand, R. L. Serotonin release and uptake in the gastrointestinal tract. *Auton Neurosci*. **153**, 47–57 <https://doi.org/10.1016/j.autneu.2009.08.002> (2010).
5. Graeme-Cook, F. in *Surgical Pathology of the GI Tract, Liver, Biliary Tract, and Pancreas* (Second Edition) (eds Robert D. Odze & John R. Goldblum) 653–680(W.B. Saunders, 2009).

6. Halperin, D. M. *et al.* Frequency of carcinoid syndrome at neuroendocrine tumour diagnosis: a population-based study. *Lancet Oncol.* **18**, 525–534 [https://doi.org/10.1016/S1470-2045\(17\)30110-9](https://doi.org/10.1016/S1470-2045(17)30110-9) (2017).
7. National Comprehensive Cancer Network. Clinical Practice Guidelines in Oncology Neuroendocrine and Adrenal Tumors (version 1.2019). (2019).
8. Cives, M., Soares, H. P. & Strosberg, J. Will clinical heterogeneity of neuroendocrine tumors impact their management in the future? Lessons from recent trials. *Curr Opin Oncol.* **28**, 359–366 <https://doi.org/10.1097/CCO.0000000000000299> (2016).
9. Karpathakis, A. *et al.* Prognostic Impact of Novel Molecular Subtypes of Small Intestinal Neuroendocrine Tumor. *Clin Cancer Res.* **22**, 250–258 <https://doi.org/10.1158/1078-0432.CCR-15-0373> (2016).
10. Yao, J. *et al.* Genomic profiling of NETs: a comprehensive analysis of the RADIANT trials. *Endocr Relat Cancer.* **26**, 391–403 <https://doi.org/10.1530/ERC-18-0332> (2019).
11. Kulke, M. H. *et al.* High-resolution analysis of genetic alterations in small bowel carcinoid tumors reveals areas of recurrent amplification and loss. *Genes Chromosomes Cancer.* **47**, 591–603 <https://doi.org/10.1002/gcc.20561> (2008).
12. Hashemi, J. *et al.* Copy number alterations in small intestinal neuroendocrine tumors determined by array comparative genomic hybridization. *BMC Cancer.* **13**, 505 <https://doi.org/10.1186/1471-2407-13-505> (2013).
13. Francis, J. M. *et al.* Somatic mutation of CDKN1B in small intestine neuroendocrine tumors. *Nat Genet.* **45**, 1483–1486 <https://doi.org/10.1038/ng.2821> (2013).
14. Banck, M. S. *et al.* The genomic landscape of small intestine neuroendocrine tumors. *J Clin Invest.* **123**, 2502–2508 <https://doi.org/10.1172/JCI67963> (2013).
15. Wajed, S. A., Laird, P. W. & DeMeester, T. R. DNA methylation: an alternative pathway to cancer. *Ann Surg.* **234**, 10–20 <https://doi.org/10.1097/00000658-200107000-00003> (2001).
16. Esteller, M. Epigenetics in cancer. *N Engl J Med.* **358**, 1148–1159 <https://doi.org/10.1056/NEJMr072067> (2008).
17. Rauluseviciute, I., Drablos, F. & Rye, M. B. DNA hypermethylation associated with upregulated gene expression in prostate cancer demonstrates the diversity of epigenetic regulation. *BMC Med Genomics.* **13**, 6 <https://doi.org/10.1186/s12920-020-0657-6> (2020).
18. Samsom, K. G. *et al.* Molecular prognostic factors in small-intestinal neuroendocrine tumours. *Endocr Connect.* **8**, 906–922 <https://doi.org/10.1530/EC-19-0206> (2019).
19. Kim, D. H. *et al.* Allelic alterations in well-differentiated neuroendocrine tumors (carcinoid tumors) identified by genome-wide single nucleotide polymorphism analysis and comparison with pancreatic endocrine tumors. *Gene Chromosome Canc.* **47**, 84–92 <https://doi.org/10.1002/gcc.20510> (2008).
20. Tian, Y. *et al.* ChAMP: updated methylation analysis pipeline for Illumina BeadChips. *Bioinformatics.* **33**, 3982–3984 <https://doi.org/10.1093/bioinformatics/btx513> (2017).

21. George, J. W. *et al.* Integrated Epigenome, Exome, and Transcriptome Analyses Reveal Molecular Subtypes and Homeotic Transformation in Uterine Fibroids. *Cell Rep* **29**, 4069–4085 e4066, doi:10.1016/j.celrep.2019.11.077 (2019).
22. Kamburov, A., Stelzl, U., Lehrach, H. & Herwig, R. The ConsensusPathDB interaction database: 2013 update. *Nucleic Acids Res.* **41**, D793–800 <https://doi.org/10.1093/nar/gks1055> (2013).
23. Yang, X., Li, J., Lee, Y. & Lussier, Y. A. GO-Module: functional synthesis and improved interpretation of Gene Ontology patterns. *Bioinformatics.* **27**, 1444–1446 <https://doi.org/10.1093/bioinformatics/btr142> (2011).
24. Szklarczyk, D. *et al.* The STRING database in 2017: quality-controlled protein-protein association networks, made broadly accessible. *Nucleic Acids Res.* **45**, D362–D368 <https://doi.org/10.1093/nar/gkw937> (2017).
25. Shannon, P. *et al.* Cytoscape: a software environment for integrated models of biomolecular interaction networks. *Genome Res.* **13**, 2498–2504 <https://doi.org/10.1101/gr.1239303> (2003).
26. Edfeldt, K. *et al.* TCEB3C a putative tumor suppressor gene of small intestinal neuroendocrine tumors. *Endocr Relat Cancer.* **21**, 275–284 <https://doi.org/10.1530/ERC-13-0419> (2014).
27. Kim, D. H. *et al.* Allelic alterations in well-differentiated neuroendocrine tumors (carcinoid tumors) identified by genome-wide single nucleotide polymorphism analysis and comparison with pancreatic endocrine tumors. *Genes Chromosomes Cancer.* **47**, 84–92 <https://doi.org/10.1002/gcc.20510> (2008).
28. Wang, G. G. *et al.* Comparison of genetic alterations in neuroendocrine tumors: frequent loss of chromosome 18 in ileal carcinoid tumors. *Mod Pathol.* **18**, 1079–1087 <https://doi.org/10.1038/modpathol.3800389> (2005).
29. Gad, A. A. & Balenga, N. The Emerging Role of Adhesion GPCRs in Cancer. *ACS Pharmacol Transl Sci.* **3**, 29–42 <https://doi.org/10.1021/acspstsci.9b00093> (2020).
30. Singh, A., Nunes, J. J. & Ateeq, B. Role and therapeutic potential of G-protein coupled receptors in breast cancer progression and metastases. *Eur J Pharmacol.* **763**, 178–183 <https://doi.org/10.1016/j.ejphar.2015.05.011> (2015).
31. Khalil, B. D. *et al.* GPCR Signaling Mediates Tumor Metastasis via PI3Kbeta. *Cancer Res.* **76**, 2944–2953 <https://doi.org/10.1158/0008-5472.CAN-15-1675> (2016).
32. Xing, M. *et al.* Methylation of the thyroid-stimulating hormone receptor gene in epithelial thyroid tumors: a marker of malignancy and a cause of gene silencing. *Cancer Res.* **63**, 2316–2321 (2003).
33. Shi, X., Li, X., Chen, L. & Wang, C. Analysis of somatostatin receptors and somatostatin promoter methylation in human gastric cancer. *Oncol Lett.* **6**, 1794–1798 <https://doi.org/10.3892/ol.2013.1614> (2013).
34. Chen, B. H. *et al.* New insights into long noncoding RNAs and pseudogenes in prognosis of renal cell carcinoma. *Cancer Cell Int* **18**, doi:ARTN 157. 10.1186/s12935-018-0652-6 (2018).
35. Wu, C. *et al.* Identification of cancer-related potential biomarkers based on lncRNA-pseudogene-mRNA competitive networks. *Febs Lett.* **592**, 973–986 <https://doi.org/10.1002/1873-3468.13011>

(2018).

36. Stewart, G. L. *et al.* Aberrant Expression of Pseudogene-Derived lncRNAs as an Alternative Mechanism of Cancer Gene Regulation in Lung Adenocarcinoma. *Front Genet.* **10**, 138 <https://doi.org/10.3389/fgene.2019.00138> (2019).
37. Lian, Y. *et al.* The pseudogene derived from long non-coding RNA DUXAP10 promotes colorectal cancer cell growth through epigenetically silencing of p21 and PTEN. *Sci Rep.* **7**, 7312 <https://doi.org/10.1038/s41598-017-07954-7> (2017).
38. Cornwell, A. C. & Feigin, M. E. Unintended Effects of GPCR-Targeted Drugs on the Cancer Phenotype. *Trends Pharmacol Sci.* **41**, 1006–1022 <https://doi.org/10.1016/j.tips.2020.10.001> (2020).
39. Sriram, K. & Insel, P. A. G Protein-Coupled Receptors as Targets for Approved Drugs: How Many Targets and How Many Drugs? *Mol Pharmacol.* **93**, 251–258 <https://doi.org/10.1124/mol.117.1111062> (2018).
40. Dorsam, R. T. & Gutkind, J. S. G-protein-coupled receptors and cancer. *Nat Rev Cancer.* **7**, 79–94 <https://doi.org/10.1038/nrc2069> (2007).
41. Cui, T. *et al.* Olfactory receptor 51E1 protein as a potential novel tissue biomarker for small intestine neuroendocrine carcinomas. *Eur J Endocrinol.* **168**, 253–261 <https://doi.org/10.1530/EJE-12-0814> (2013).
42. Drozdov, I. *et al.* Gene network inference and biochemical assessment delineates GPCR pathways and CREB targets in small intestinal neuroendocrine neoplasia. *PLoS One.* **6**, e22457 <https://doi.org/10.1371/journal.pone.0022457> (2011).

Figures

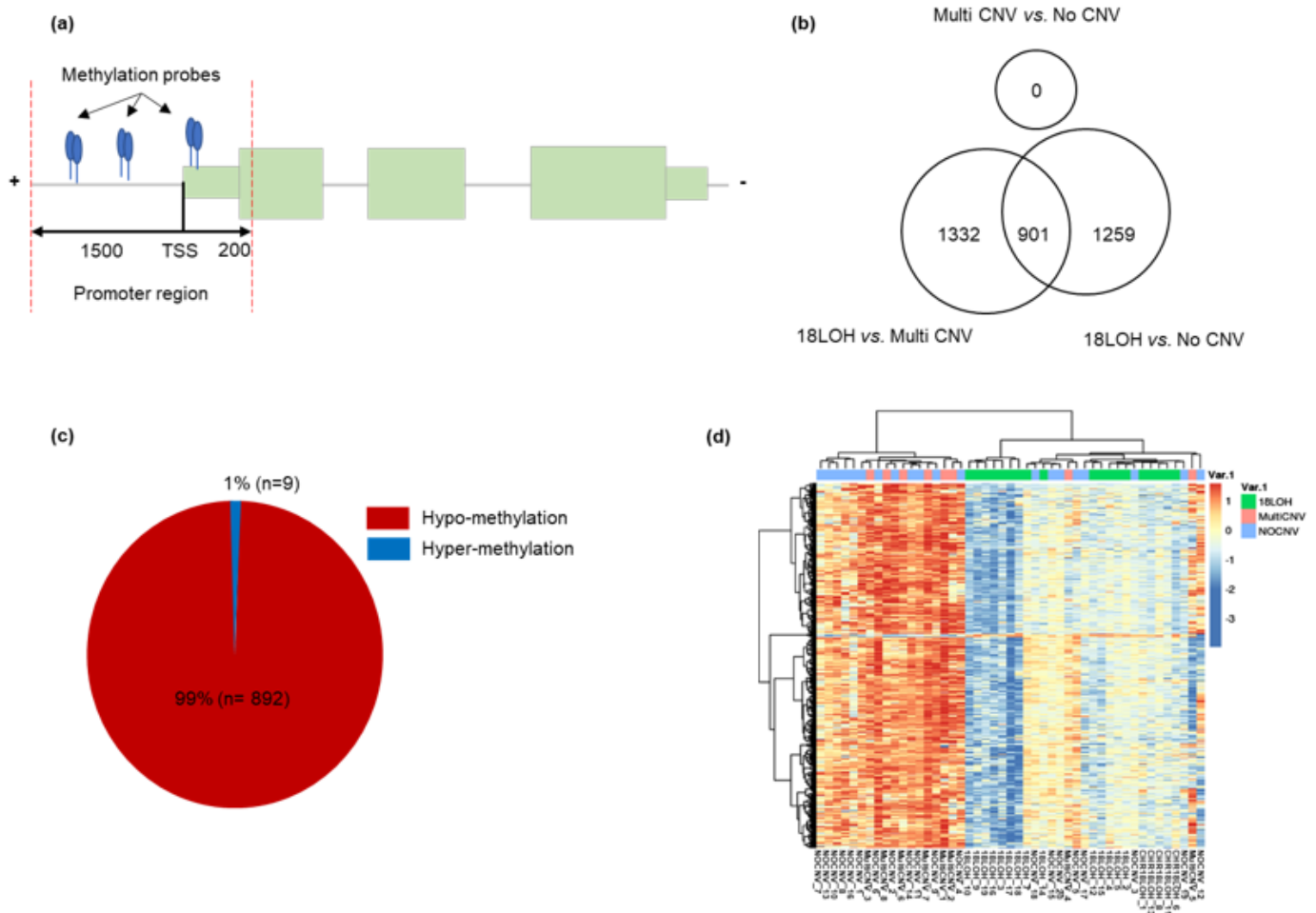


Figure 2

Differential methylation status between molecular subtypes. (a) A schema methylation probes within promoter region. Methylation probes between -1500bp and 200bp from the transcript start site are considered. (b) The number of significantly differential methylation genes of each comparison. The overlapped differential methylation of 18LOH vs. Multi CNV and 18LOH vs. No CNV is considered as 901 genes specific to 18LOH. (c) Proportion of hypomethylated (n=892, 99%) and hypermethylated (n=9, 1%) genes in 18LOH tumors. (d) Heatmap of 901 differentially methylated genes for each tumor. Blue indicates hypomethylation. Red indicates hypermethylation. Tumor molecular subtypes are indicated in green (18LOH), pink (multiCNV) or blue (NoCNV).

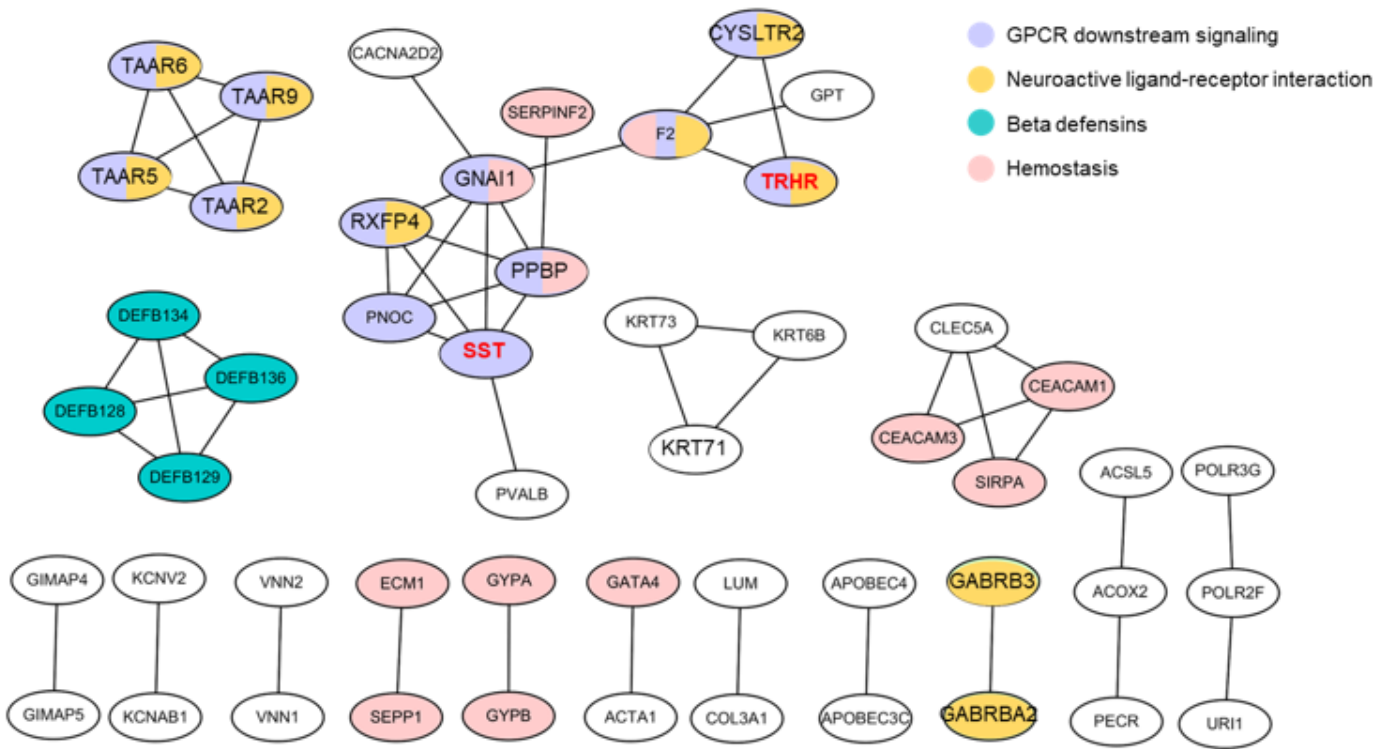


Figure 3

Protein-protein interaction network of 901 genes with differential methylation in 18LOH group. Protein-protein interaction network was constructed using interactions with highest confidence > 0.9 (51 genes). Four enriched functional pathways were identified and genes assigned to these pathways are patterned: GPCR signaling (purple); Neuroactive ligand-receptor interaction (yellow); Beta-defensins (green) and Hemostasis (pink). If gene is assigned to multiple networks, the circle is multiple patterns.

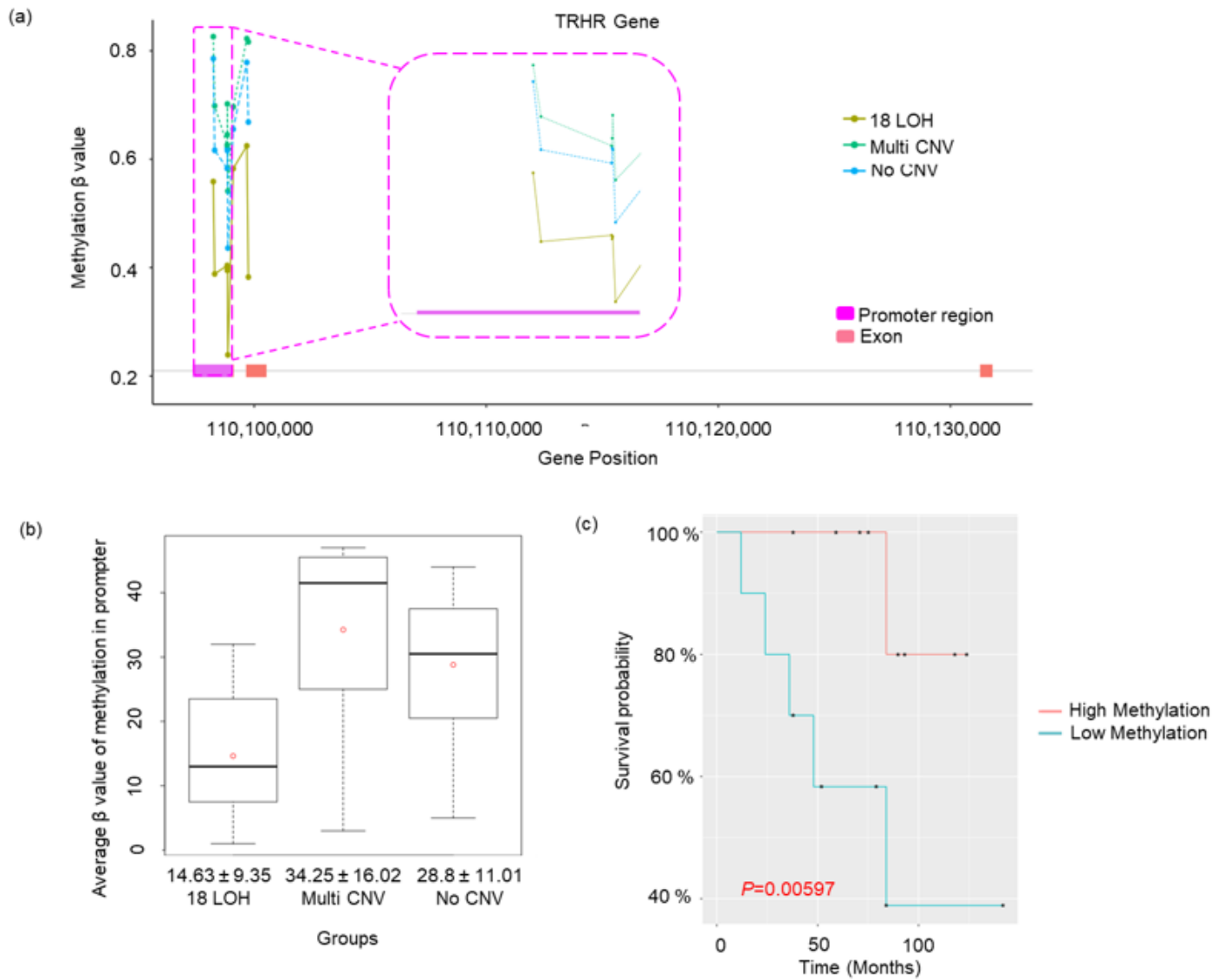


Figure 4

Methylation status of TRHR gene promoter. (a) A plot of beta-values of methylation probes within the promoter (Y-axis) and genomic coordinates (X-axis). The promoter region (pink), exon (orange) and intron are presented a bottom line of the graph. (b) A boxplot including distributions of average beta-value of methylation probes in the promoter for each molecular subtype. (c) Survival analysis comparing 18LOH tumors with high methylation (red line; samples 18LOH_2, _4, _5, _6, _7, _9, _14, _15, _16) and low methylation (blue line; samples 18LOH_1, _3, _8, _10, _11, _12, _13, _17, _18, _19) of TRHR promoter.

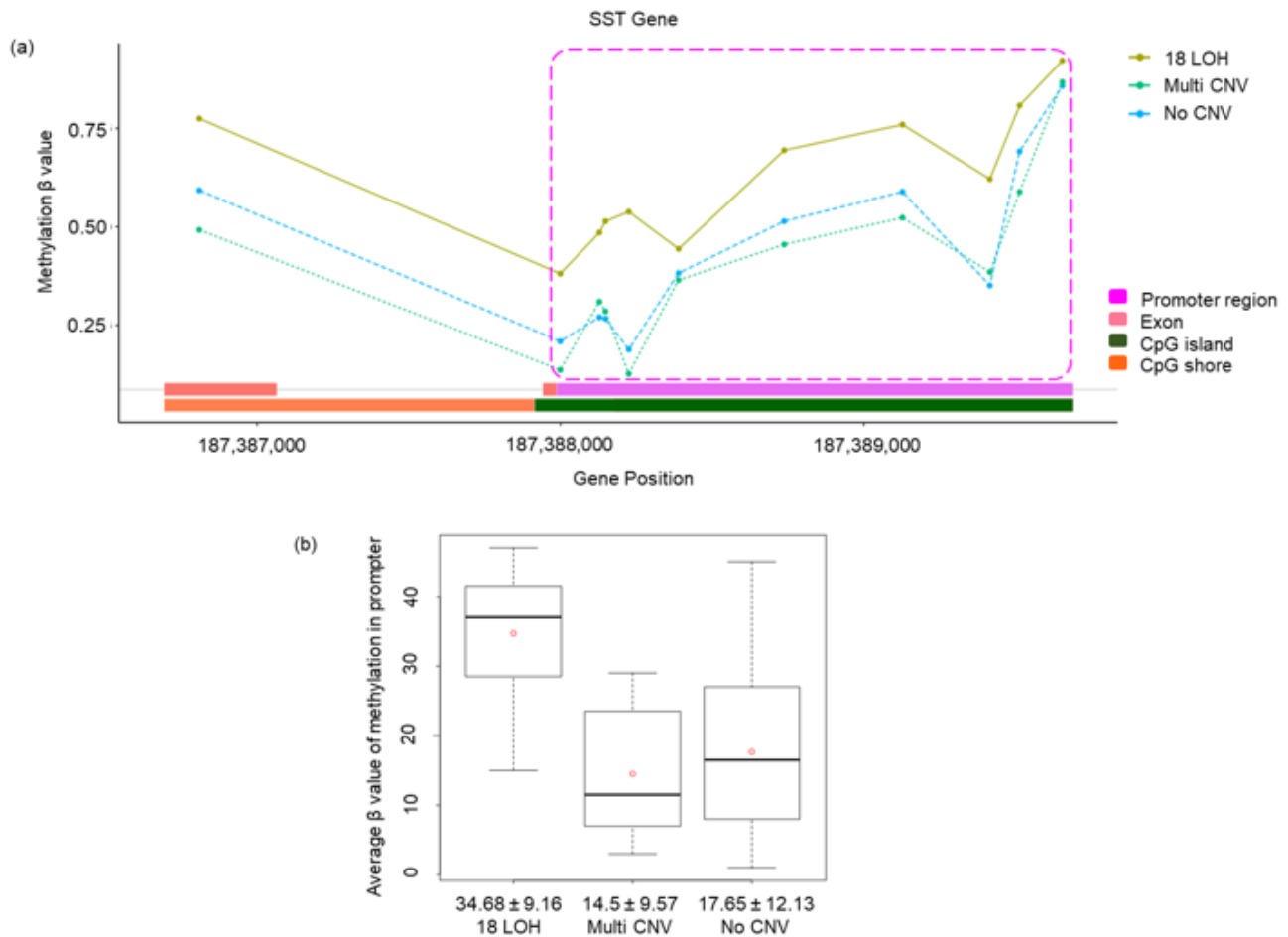


Figure 5

Methylation status in the SST gene promoter. (a) A plot of beta-values of methylation probes within the promoter (Y-axis) and genomic coordinates (X-axis). The promoter region (pink), exon (orange), intron, CpG island (green), and shore (dark orange) are presented a bottom line of the graph. (b) A boxplot including distributions of average beta-value of methylation probes in the promoter for each molecular subtype.

Supplementary Files

This is a list of supplementary files associated with this preprint. Click to download.

- [SupplementaryFigures13v2.pdf](#)
- [Supplementarytable120210209.xlsx](#)